Inorg. Chem. **2006**, *45*, 3086–3096

Proton-Transfer and H_2-Elimination Reactions of Main-Group Hydrides EH_4^- (E = B, Al, Ga) with Alcohols

Oleg A. Filippov,[†] Andrey M. Filin,[†] Viktoria N. Tsupreva,[†] Natalia V. Belkova,[†] Agustí Lledós,*[,‡] Gregori Ujaque,[‡] Lina M. Epstein,*[,†] and Elena S. Shubina*[,†]

A. N. Nesmeyanov Institute of Organoelement Compounds, Russian Academy of Sciences, 28 Vavilov strasse, 119991 Moscow, Russia, and Departament de Química, Edifici Cn, Universitat Autònoma de Barcelona, 08193 Bellaterra, Catalonia, Spain

Received November 24, 2005

The reaction of the isostructural anions of group 13 hydrides EH_4^- (E = B, Al, Ga) with proton donors of different strength (CH_3OH, CF_3CH_2OH, and CF_3OH) was studied with different theoretical methods [DFT/B3LYP and second-order Møller–Plesset (MP2) using the 6-311++G(d,p) basis set]. The results show the general mechanism of the reaction: the dihydrogen-bonded (DHB) adduct (EH···HO) formation leads through the activation barrier to the next concerted step of H_2 elimination and alkoxo product formation. The structures, interaction energies (calculated by different approaches including the energy decomposition analysis), vibrational E–H modes, and electron-density distributions were analyzed for all of the DHB adducts. The transition state (TS) is the dihydrogen complex stabilized by a hydrogen bond with the anion [$EH_3(\eta^2\text{-}H_2)\cdots OR^-$]. The single exception is the reaction of BH_4^- with CF_3OH exhibiting two TSs separated by a shallow minimum of the $BH_3(\eta^2\text{-}H_2)\cdots OR^-$ intermediate. The structures and energies of all of the species were calculated, leading to the establishment of the potential energy profiles for the reaction. A comparison is made with the mechanism of the proton-transfer reaction to transition-metal hydrides. The solvent influence on the stability of all of the species along the reaction pathway was accounted for by means of polarizable conductor calculation model calculations in tetrahydrofuran (THF). Although in THF the DHB intermediates, the TSs, and the products are destabilized with respect to the separated reactants, the energy barriers for the proton transfer are only slightly affected by the solvent. The dependence of the energies of the DHB complexes, TSs, and products as well as the energy barriers for the H_2 release on the central atom and the proton donor strength is also discussed.

Introduction

Proton-transfer reactions to transition-metal hydrides have been intensively studied in recent years.[1] The structures of the proton-transfer intermediates have been elucidated, and the potential energy surface has been thoroughly explored.[2] It was well established that the dihydrogen complex [M](η^2-H_2) is the direct product of the proton transfer to the hydride site[3] and that the formation of a dihydrogen-bonded (DHB) adduct M−H···HA[4] is the first stage in the protonation pathway of a transition-metal hydride.[5] In some cases, the coordinated dihydrogen molecule formed is easily released, and the alkoxo derivative [M]OR is the final product.[6] Alcohols of different acidity are frequently used to probe the acid−base reactions.[7] The use of fluorinated alcohols

* To whom correspondence should be addressed. E-mail: shu@ineos.ac.ru. Fax: +7 495 1355085.
[†] Russian Academy of Sciences.
[‡] Universitat Autònoma de Barcelona.

(1) Peruzzini, M.; Poli, R. *Recent Advances in Hydride Chemistry*; Elsevier: Amsterdam, The Netherlands, 2001.
(2) Belkova, N. V.; Shubina, E. S.; Epstein, L. M. *Acc. Chem. Res.* **2005**, *38*, 624−631.
(3) Kubas, G. J. *Metal Dihydrogen and σ-Bond Complexes*; Kluwer Academic/Plenum: New York, 2001.
(4) Crabtree, R. H.; Siegbahn, P. E. M.; Eisenstein, O.; Rheingold, A. L.; Koetzle, T. F. *Acc. Chem. Res.* **1996**, *29*, 348−354.
(5) (a) Morris, R. H. In *Recent Advances in Hydride Chemistry*; Peruzzini, M.; Poli, R., Eds.; Elsevier: Amsterdam, The Netherlands, 2001; pp 1−38. (b) Epstein, L. M.; Belkova, N. V.; Shubina, E. S. In *Recent Advances in Hydride Chemistry*; Peruzzini, M., Poli, R., Eds.; Elsevier: Amsterdam, The Netherlands, 2001; pp 391−418. (c) Epstein, L. M.; Shubina, E. *Coord. Chem. Rev.* **2002**, *231*, 165−181. (d) Bahkmutov, V. I. *Eur. J. Inorg. Chem.* **2005**, 245−255.
(6) Belkova, N. V.; Besora, M.; Epstein, L. M.; Lledós, A.; Maseras, F.; Shubina, E. S. *J. Am. Chem. Soc.* **2003**, *25*, 7715−7725.
(7) Harañczyk, M.; Rak, J.; Gutowski, M.; Radisic, D.; Stokes, S. T.; Bowen, K. H. *J. Phys. Chem. B* **2005**, *109*, 13383−13391.

10.1021/ic052028n CCC: $33.50
Published on Web 03/02/2006

appeared to be particularly helpful in the study of the kinetics of proton transfer to transition-metal hydrides, allowing one to control the reaction rate depending on the proton donor acidity.[6,8,9]

In recent years, the interest in main-group metal hydrides has considerably risen.[10] One of the main reasons behind this interest is their potentiality for the storage and production of hydrogen.[11] However, the proton-transfer reactions to main-group hydrides have been much less explored than those to transition-metal hydrides. The ability of main-group hydrides to form dihydrogen bonds, initially studied by experimental and theoretical methods for boron hydrides,[12,13] has then been extended to other main-group hydrides, in particular to those of group 13 elements.[14] Several theoretical studies of the dihydrogen bond between simple hydrides and proton donors (for example, LiH, BeH_2, MgH_2, BH_3, and AlH_3 and HF, H_2O, and NH_3) have been published.[15] These studies have largely contributed to the understanding of the nature of the H···H interactions.[16] We recently reported a theoretical and variable-temperature IR investigation of the DHB adduct formed in low-polar solvents between GaH_4^- and weak XH acids, including CF_3CH_2OH (trifluoroethanol, TFE) and CH_3OH.[17]

Alkoxoaluminum and gallium hydrides of the types H_2MOR and $HM(OR)_2$ have been synthesized by the reaction of alane and gallane adducts $LiAlH_4$ or $H_3M{\cdot}OEt_2$ with ROH[18] accompanied by H_2 release. This behavior suggests that the reaction takes place with a mechanism similar to that reported for transition-metal hydride protonation. Other

Scheme 1

$$EH_4^- + HOR \rightleftharpoons [H_3EH...HOR]^- \rightleftharpoons [H_3E(\eta^2\text{-}H_2)\cdots OR]^- \longrightarrow [H_3EOR]^- + H_2$$

1 2 3 4

examples of the tetrahydride alcoholysis/hydrolysis reactions have been reported, in particular for the AlH_4^-,[19−21] BH_4^-,[22] and GaH_4^-[23] hydrides. However, the possibility of EH···HOR DHB intermediates along the reaction pathway had not been considered at that time. The experimental study of the hydrolysis of BH_4^- in H_2O[24] and the solid-state decomposition of the DHB complexes $LiBH_4$·triethanolamine[25] have been reported; to the best of our knowledge, these are the only studies involving the determination of the reaction activation parameters that can be found in the literature. Recently, the structures and decomposition paths of complexes between AlH_4^- and three proton donors (H_2O, HF, and HCl) have been studied by ab initio methods.[26]

By analogy with transition-metal hydrides,[2,6,8,9] we could suggest that in the reaction of group 13 hydrides with alcohols the proton transfer from the DHB complex leads in a first step to the nonclassical (η^2-H_2) complex formation, which is then followed by H_2 elimination to yield the alkoxo product[17] (Scheme 1).

However, in contrast to transition metals, the main-group metal centers are not well suited for back-donation of electron density through a π-type interaction between a filled metal orbital and the empty σ_{H_2}*.[27] For this reason, main-group (η^2-H_2) complexes should be very unstable. Indeed, dihydrogen binds only weakly to main-group metals, forming complexes that have no more than a transient existence under normal conditions.[10] The $BH_3(\eta^2\text{-}H_2)$ complex has been detected (IR spectra in cryogenic matrixes at 13−27 K), and its binding energy has been calculated to be about 1.5 kcal/mol.[28] There are no clear spectroscopic signs of $AlH_3(\eta^2\text{-}H_2)$,[10] which is predicted to be slightly more strongly bound than $BH_3(\eta^2\text{-}H_2)$.[27] The limited stability of the main-group (η^2-H_2) complexes may affect the proton-transfer mechanism. Here we present a theoretical study devoted to the reactions of the EH_4^- hydrides with alcohols of different strength as proton donors, which for the first time considers all three group 13 elements (B, Al, and Ga) in the same study. The

(8) (a) Belkova, N. V.; Revin, P. O.; Epstein, L. M.; Vorontsov, E. V.; Bakhmutov, V. I.; Shubina, E. S.; Collange, E.; Poli, R. *J. Am. Chem Soc.* **2003**, *125*, 11106−11115. (b) Belkova, N. V.; Collange, E.; Dub, P.; Epstein, L. M.; Lemenovskii, D. A.; Lledós, A.; Maresca, O.; Maseras, F.; Poli, R.; Revin, P. O.; Shubina, E. S.; Vorontsov, E. V. *Chem.—Eur. J.* **2005**, *11*, 873−888.

(9) Bakhmutova, E.; Bakhmutov, V. I.; Belkova, N. V.; Besora, M.; Epstein, L. M.; Lledós, A.; Nikonov, G.; Shubina, E. S.; Tomàs, J.; Vorontsov, E. V. *Chem.—Eur. J.* **2004**, *10*, 661−671.

(10) Aldridge, S.; Downs, A. J. *Chem. Rev.* **2001**, *101*, 3305−3365.

(11) Grochala, W.; Edwards, P. P. *Chem. Rev.* **2004**, *104*, 1283−1315.

(12) Richardson, T. B.; de Gala, S.; Crabtree, R. H.; Siegbahn, P. E. M. *J. Am. Chem. Soc.* **1995**, *117*, 12875−12876.

(13) (a) Shubina, E. S.; Bakhmutova, E. V.; Saitkulova, L. N. Epstein, L. M. *Mendeleev Commun.* **1997**, 83−84. (b) Epstein, L. M.; Shubina, E. S.; Bakhmutova, E. V.; Saitkulova, L. N.; Bakhmutov, V. I.; Gambaryan, N. P.; Chistyakov, A. L.; Stankevich, I. V. *Inorg. Chem.* **1998**, *37*, 3013−3017. (c) Shubina, E. S.; Belkova, N. V.; Bakhmutova, E. V.; Saitkulova, L. N.; Ionidis, A. V.; Epstein L. M. *Russ. Chem. Bull.* **1998**, *47*, 846−851.

(14) Custelcean, R.; Jackson, J. E. *Chem. Rev.* **2001**, *101*, 1963−1983.

(15) (a) Kulkarni, S. A. *J. Phys. Chem. A* **1998**, *102*, 7704−7711. (b) Kulkarni, S. A.; Srivastava, A. K. *J. Phys. Chem. A* **1999**, *103*, 2836−2842. (c) Kulkarni, S. A. *J. Phys. Chem. A* **1999**, *103*, 9330−9335.

(16) (a) Alkorta, I.; Elguero, J.; Mo, O.; Yañez, M.; Del Bene, J. *J. Phys. Chem. A* **2002**, *106*, 9325−9330. (b) Grabowski, S. J.; Sokalski, W. A.; Leszczynski, J. *J. Phys. Chem. A* **2004**, *108*, 5823−5830. (c) Grabowski, S. J.; Sokalski, W. A.; Leszczynski, J. *J. Phys. Chem. A* **2005**, *109*, 4331−4341.

(17) Belkova, N. V.; Filippov, O. A.; Filin, A. M.; Teplitskaya, L. N.; Shmyrova, Y. V.; Gavrilenko, V. V.; Golubinskaya, L. M.; Bregadze, V. I.; Epstein, L. M.; Shubina, E. S. *Eur. J. Inorg. Chem.* **2004**, 3453−3461.

(18) (a) Cesari, M. *Gazz. Chim. Ital.* **1980**, *110*, 365. (b) Koutsantonis, G. A.; Lee, F. C.; Raston, C. L. *Main Group Chem.* **1995**, *1*, 21−28. (c) Veith, M.; Faber, S.; Wolfanger, H.; Huch, V. *Chem. Ber.* **1996**, *129*, 381−384. (d) Gradiner, M. G.; Koutsantonis, G. A.; Lawrence, S. M.; Nichols, P. J.; Raston, C. L. *J. Chem. Soc., Chem. Commun.* **1996**, 2035−2036.

(19) Brown, H. C.; Garg, C. P. *J. Am. Chem Soc.* **1964**, *86*, 1079−1085.

(20) Zakharkin, L. I.; Maslin, D. N.; Gavrilenko, V. V. *Russ. J. Gen. Chem.* **1966**, *36*, 200−206.

(21) Turova, N. Y.; Karpovskaya, M. I.; Novoselova, A. V.; Bakum, S. I. *Inorg. Chim. Acta* **1977**, *21*, 157−161.

(22) Golden, J.; Schreier, C.; Singaram, B.; Williamson, S. *Inorg. Chem.* **1992**, *31*, 1533−1535.

(23) Gavrilenko, V. V.; Kolesov, V. S.; Zakharkin, L. I. *Russ. Chem. Bull.* **1984**, *33*, 2533−2535.

(24) Mesmer, R. E.; Jolly, W. L. *Inorg. Chem.* **1962**, *1*, 608−612.

(25) (a) Custelcean, R.; Jackson, J. E. *Angew. Chem., Int. Ed.* **1999**, *38*, 1661−1663. (b) Custelcean, R.; Jackson, J. E. *Angew. Chem., Int. Ed.* **2000**, *39*, 3299−3302. (c) Custelcean, R.; Jackson, J. E. *J. Am. Chem. Soc.* **2000**, *122*, 5251−5257. (d) Custelcean, R.; Jackson, J. E. *Thermochim. Acta* **2002**, *388*, 143−150.

(26) Marincean, S.; Jackson, J. E. *J. Phys. Chem. A* **2004**, *108*, 5521−5526.

(27) Maseras, F.; Lledós, A.; Clot, E.; Eisenstein, O. *Chem. Rev.* **2000**, *100*, 601−636.

(28) (a) Tague, T. J., Jr.; Andrews, L. *J. Am. Chem. Soc.* **1994**, *116*, 4970−4976. (b) Watts, J. D.; Bartlett, R. J. *J. Am. Chem. Soc.* **1995**, *117*, 825−826. (c) Schreiner, P. R.; Schaefer, H. F.; Schleyer, P. v. R. *J. Chem. Phys.* **1994**, *101*, 7625−7632.

aim of the present work is to determine the reaction mechanism for H_2 elimination and alkoxo derivative formation, to elucidate the dependence of the alcoholysis potential energy profile on the central element and on the acidity of the proton donor, and to analyze the trends across the group.

Computational Details

Full geometry optimizations were carried out with *Gaussian03*[30] package at the density functional theory (DFT) level using the a hybrid B3LYP functional[31] and at the second-order Møller−Plesset[32] perturbation theory (MP2) level. The 6-311++G(d,p) basis set was used for all of the atoms. As was shown in the previous calculations of BH_4^-/GaH_4^- interaction with proton donors,[17] the 6-311G(d,p) and 6-311++G(d,p) basis sets give similar results for gallium, but only the 6-311++G(d,p) basis set gives good agreement with experimental data for boron derivatives. The nature of all of the stationary points on the potential energy surfaces was confirmed by a vibrational analysis. Intrinsic reaction coordinate (IRC) calculations were carried out in both directions starting from the located transition states (TSs). The gas-phase complexation energies were corrected from the basis set superposition error according to the counterpoise method of Boys and Bernardi.[33]

Natural atomic charges and Wiberg bond indices[34] were calculated at the B3LYP/6-311++G(d,p) level by using the natural bond orbital (NBO) analysis[35] option as incorporated in *Gaussian03*.

Topological analysis of the electron-density distribution function $\rho(r)$ was performed using the *AIMPAC program package*[36] based on the wave function obtained by the B3LYP calculations. The energy of the H···H interactions was estimated using the correlation between the energy of the contact (E_{HH}) with the value of the potential energy density function $V(r)$ in the corresponding bond critical point (3, −1).[37]

Solvent effects were taken into account by means of the polarizable conductor calculation model (CPCM),[38] using standard options.[30] The solvation free energies were computed in tetrahydrofuran (THF; $\epsilon = 7.58$) at the gas-phase-optimized geometries. Test calculations on the influence of the geometry optimization in the THF energies were also carried out.

The Kitaura−Morokuma energy decomposition analysis (EDA)[39] of the DHB energy contributions was performed using the PC GAMESS version[40a] of the GAMESS (U.S.) QC package.[40b] Because of the program limitations, the 6-31++G(d,p) basis set was used for structure optimizations and EDA calculations instead of 6-311++G(d,p), which is not applicable to the gallium atom in PC GAMESS.

Results and Discussion

The reaction between the group 13 hydrides (BH_4^-, AlH_4^-, and GaH_4^-) and several alcohols with different proton donor strength (CH_3OH, TFE, and CF_3OH) to release molecular hydrogen and form the alkoxo compounds H_3EOR has been theoretically analyzed by B3LYP/6-311++G(d,p) and compared to the available experimental data. DFT results have been backed with MP2 calculations. MP2 computations for the reaction of BH_4^- with CH_3OH and CF_3OH using the 6-311++G(d,p) basis set gave results similar to the B3LYP ones. Therefore, all of the data discussed within the paper come from the B3LYP/6-311++G(d,p) calculations unless specified otherwise. The results obtained are presented in two main subsections. The first one is devoted to the analysis of the DHB structures initially formed between the hydrides and alcohols. The second subsection deals with the reaction mechanisms for the alkoxo formation and H_2 elimination that take place after the initial DHB intermediate is formed.

I. Characterization of the $[H_3EH]^-$···HOR DHB Intermediates. The analysis of several properties of the initial DHB intermediates formed in the reaction of group 13 hydrides with alcohols was performed. The first part covers the structural analysis of the DHB complexes. Next, two subsections are devoted to the electron density and energy analysis of the DHB interaction for these systems. In the last subsection, a vibrational analysis is presented and compared to the experimental IR frequencies. Although preliminary results on GaH_4^- and BH_4^- adducts have already been published,[17] the study presented in this section for the whole set of hydrides and alcohols will allow for a comparison among the group 13 elements.

Structural Analysis. The first step of the reaction between the group 13 hydrides and the set of alcohols considered in this study is the formation of a DHB adduct. The geometries of EH_4^-·HOR (E = B, Al, Ga; R = CH_3, CF_3, CF_3CH_2) species have been fully optimized. As an example, Figure 1 shows the DHB complex formed between AlH_4^- and CF_3CHOH. In all of the cases, the EH···HO distance found is shorter than the sum of the van der Waals (vdW) radii

(29) Schreiner, P. R.; Schaefer, H. F.; Schleyer, P. v. R. *J. Chem. Phys.* **1995**, *103*, 5565−5569.

(30) Frisch, M. J.; Trucks, G. W.; Schlegel, H. B.; Scuseria, G. E.; Robb, M. A.; Cheeseman, J. R.; Montgomery, J. A., Jr.; Vreven, T.; Kudin, K. N.; Burant, J. C.; Millam, J. M.; Iyengar, S. S.; Tomasi, J.; Barone, V.; Mennucci, B.; Cossi, M.; Scalmani, G.; Rega, N.; Petersson, G. A.; Nakatsuji, H.; Hada, M.; Ehara, M.; Toyota, K.; Fukuda, R.; Hasegawa, J.; Ishida, M.; Nakajima, T.; Honda, Y.; Kitao, O.; Nakai, H.; Klene, M.; Li, X.; Knox, J. E.; Hratchian, H. P.; Cross, J. B.; Bakken, V.; Adamo, C.; Jaramillo, J.; Gomperts, R.; Stratmann, R. E.; Yazyev, O.; Austin, A. J.; Cammi, R.; Pomelli, C.; Ochterski, J. W.; Ayala, P. Y.; Morokuma, K.; Voth, G. A.; Salvador, P.; Dannenberg, J. J.; Zakrzewski, V. G.; Dapprich, S.; Daniels, A. D.; Strain, M. C.; Farkas, O.; Malick, D. K.; Rabuck, A. D.; Raghavachari, K.; Foresman, J. B.; Ortiz, J. V.; Cui, Q.; Baboul, A. G.; Clifford, S.; Cioslowski, J.; Stefanov, B. B.; Liu, G.; Liashenko, A.; Piskorz, P.; Komaromi, I.; Martin, R. L.; Fox, D. J.; Keith, T.; Al-Laham, M. A.; Peng, C. Y.; Nanayakkara, A.; Challacombe, M.; Gill, P. M. W.; Johnson, B.; Chen, W.; Wong, M. W.; Gonzalez, C.; Pople, J. A. *Gaussian 03*, revision C.02; Gaussian, Inc.: Wallingford, CT, 2004.

(31) (a) Becke, A. D. *J. Chem. Phys.* **1993**, *98*, 5648−5652. (b) Stephens, P. J.; Devlin, J. F.; Chabalowski, C. F.; Frisch, M. J. *J. Phys. Chem.* **1994**, *98*, 11623−11627.

(32) Moller, C.; Plesset, M. S. *Phys. Rev.* **1934**, *46*, 618−622.

(33) Boys, S. F.; Bernardi, F. *Mol. Phys.* **1970**, *19*, 553−566.

(34) Wiberg, K. *Tetrahedron* **1968**, *24*, 1083−1096.

(35) Reed, A. E.; Curtiss, L. A.; Weinhold, F. *Chem. Rev.* **1988**, *88*, 899−926.

(36) Cheeseman, J.; Keith, T. A.; Bader, R. W. F. *AIMPAC program package*; McMaster University: Hamilton, Ontario, Canada, 1992.

(37) (a) Espinosa, E.; Molins, E.; Lecomte, C. *Chem. Phys. Lett.* **1998**, *285*, 170−173. (b) Espinosa, E.; Alkorta, I.; Rozas, I.; Elguero, J.; Molins, E. *Chem. Phys. Lett.* **2001**, *336*, 457−461.

(38) (a) Barone, V.; Cossi, M. *J. Phys. Chem. A* **1998**, *102*, 1995−2001. (b) Cossi, M.; Rega, N.; Scalmani, G.; Barone, V. *J. Comput. Chem.* **2003**, *24*, 669−681.

(39) (a) Kitaura, K.; Morokuma, K. *Int. J. Quantum Chem.* **1976**, *10*, 325−331. (b) Morokuma, K.; Kitaura, K. *Chemical Applications of Atomic and Molecular Electrostatic Potentials*; Politzer, P., Truhlar, D. G., Eds.; Plenum Press: New York, 1981.

(40) (a) Granovsky, A. A. www http://classic.chem.msu.su/gran/gamess/index.html. (b) Schmidt, M. W.; Baldridge, K. K.; Boatz, J. A.; Elbert, S. T.; Gordon, M. S.; Jensen, J. H.; Koseki, S.; Matsunaga, N.; Nguyen, K. A.; Su, S.; Windus, T. L.; Dupuis, M.; Montgomery, J. A. *J. Comput. Chem.* **1993**, *14*, 1347−1363.

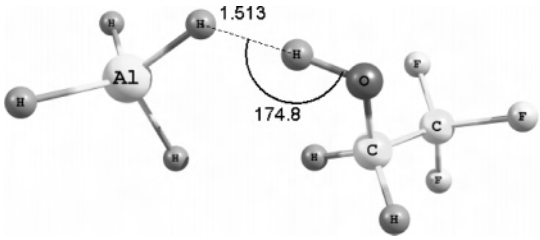

Figure 1. Structure of the DHB complex $H_3AlH\cdots HOCH_2CF_3$.

Table 1. H···H Distances (in Angstroms), H···HO Angles (in Degrees), E−H and O−H Bond Lengths (in Angstroms) in DHB Complexes and Their Elongations (ΔR, in Parentheses) with Respect to the Free Molecules

		ROH		
hydride		CH_3OH	TFE	CF_3OH
BH_4^-	*r*(H···H)	1.654	1.553	1.351
	∠H···HO	174.2	176.4	164.6
	r(B−H)	1.243 (0.005)	1.245 (0.007)	1.252 (0.014)
	r(O−H)	0.982 (0.023)	0.989 (0.025)	1.039 (0.075)
AlH_4^-	*r*(H···H)	1.622	1.513	1.258
	∠H···HO	174.0	174.8	179.2
	r(Al−H)	1.657 (0.012)	1.662 (0.017)	1.675 (0.030)
	r(O−H)	0.982 (0.023)	0.991 (0.027)	1.050 (0.086)
GaH_4^-	*r*(H···H)	1.628	1.520	1.269
	∠H···HO	174.2	175.0	178.3
	r(Ga−H)	1.638 (0.023)	1.646(0.023)	1.670 (0.047)
	r(O−H)	0.982 (0.023)	0.990 (0.026)	1.050 (0.086)

(<2.4 Å), proving the existence of an attractive interaction between the hydride and the alcohol proton.

Table 1 collects the H···H hydrogen-bond distances and the H···H−O angles as well as changes for the E−H and O−H bonds upon DHB formation. The structural parameters obtained are comparable to those observed for related DHB complexes of boron,[13b] gallium,[17] aluminum,[26] and transition-metal hydrides.[4c,6,8,9,4141] For a given alcohol, the H···H distances among the different hydrides are quite similar and decrease on going from boron to gallium and then to aluminum, indicating the increase of the H···H bond strength in the order $BH_4^- < GaH_4^- \leq AlH_4^-$.

The proton donor strength of the alcohol has a remarkable effect on the structure of the DHB adduct. For instance, in the case of BH_4^-, the H···H distances are 1.654, 1.553, and 1.351 Å for CH_3OH, TFE, and CF_3OH, respectively. The biggest change, however, is found for AlH_4^-, where the *r*(H···H) values are 1.622, 1.513, and 1.258 Å for CH_3OH, TFE, and CF_3OH, respectively; the distance variation is near 0.4 Å. Hence, the stronger the proton donor, the shorter is the H···H distance.

The H···H−O moieties are almost linear for all of the systems (angle values ranging between 165 and 178°). As expected, the E−H···H−O DHB formation entails the elongation of the proton donor (O−H) and proton acceptor (E−H) bonds. The elongation of the O−H bond increases with the proton donor capacity of the alcohol; the Δr(OH) values are close for CH_3OH and TFE, while they are much larger for CF_3OH. The O−H bond elongation is not affected by the nature of the hydride, remaining almost similar with the replacement of the central atom. The elongation of the E−H bonds is less than that of the O−H bonds and increases in the order B < Al < Ga.

A comparison of these results with those obtained using the 6-311G(d,p) basis set for DHB complexes of GaH_4^- and BH_4^- with CH_3OH and CF_3OH[17] gives similar values, indicating that the inclusion of diffuse functions has very little influence on these systems.

To explore whether the results obtained are dependent on the theoretical methodology used, MP2 calculations were performed for DHB complexes of BH_4^- and GaH_4^- with CH_3OH as well as of BH_4^- with CF_3OH using the 6-311++G(d,p) basis set. The optimized structures are similar to those obtained by DFT/B3LYP, with the H···H bond lengths being 0.04−0.12 Å longer and the interacting E−H and O−H bonds being 0.005−0.024 Å shorter in the case of MP2-optimized structures (see the Supporting Information for further details).

Finally, the structures of DHB complexes of GaH_4^- and AlH_4^- with CF_3OH were optimized in THF using the CPCM method (Figure 2). A comparison with the gas-phase data in Table 1 shows that, upon passing from the gas phase to a THF solution, the H···H distance in the DHB complexes elongates in THF by 0.097 and 0.088 Å for gallium and aluminum, respectively, while the O−H and E−H distances become shorter than those in the gas phase by 0.029−0.028 and 0.022−0.019 Å, respectively. However, the overall geometries of the DHB complexes are still very similar. These structural changes agree with a decreased DHB interaction energy in solution (see below).

Electron-Density Analysis. Upon classical hydrogen-bond formation, a certain amount of electron density transfers from the proton acceptor to the donor molecule. In addition, there are some rearrangements of density within the confines of interacting molecules, which lead to the increase in the absolute value of both the positive charge on the acidic hydrogen and the negative charge on the proton-accepting atom. A similar pattern of gain and loss of electron density has been found for DHB complexes.[8b,13b,17,41,42] In the DHB complexes studied herein, the positive NBO charge of the OH proton increases by 0.038−0.076 and the negative charge on the DHB hydride increases by 0.021−0.052. The overall charge transfer from the proton acceptor to the proton donor is 0.030−0.152 electrons, as measured by natural population analysis (Table 2).

The electron density on the H···H bond was characterized using different approaches, namely, Mulliken population analysis, NBO analysis, and Bader's "Atoms in Molecule" (AIM) theory[43] (Table 2). Mulliken overlap populations (MOPs) show the presence of electron density between two interacting hydrogen atoms but do not show a clear trend with the change of the central atom, except for the DHB complexes with CF_3OH. The MOP values increase with the

(41) Gutsul, E. I.; Belkova, N. V.; Sverdlov, M. S.; Epstein, L. M.; Shubina, E. S.; Bakhmutov, V. I.; Gribanova, T. N.; Minyaev, R. M.; Bianchini, C.; Peruzzini, M.; Zanobini, F. *Chem.—Eur. J.* **2003**, *9*, 2219−2228.
(42) Orlova, G.; Scheiner, S. *J. Phys. Chem. A* **1998**, *102*, 260−269. (b) Kar, T.; Scheiner, S. *J. Chem. Phys.* **2003**, *119*, 1473−1482.
(43) (a) Bader, R. F. W. *Atoms in Molecule, a Quantum Theory*; Clarendon Press: Oxford, U.K., 1990. (b) Bader, R. F. W. *Chem. Rev.* **1991**, *91*, 893−928.

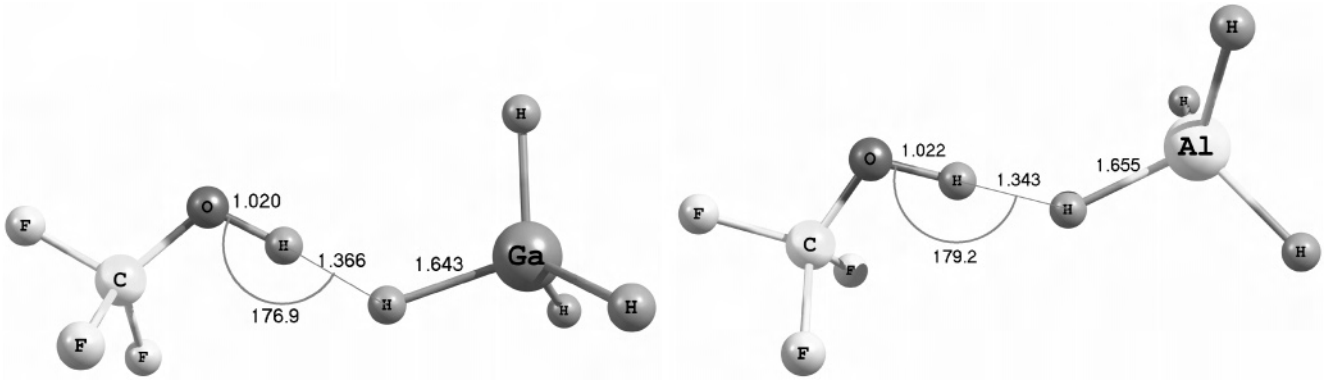

Figure 2. Structures of DHB complexes $H_3GaH\cdots HOCF_3$ and $H_3AlH\cdots HOCF_3$ optimized in THF.

Table 2. Charge Transfer (CT, in Electrons)) from EH_4^- to an Alcohol Molecule, MOPs, WBIs of H···H Bonds, and Electron Densities (ρ_c) and Laplacians ($\nabla^2\rho_c$) at the H···H Bond Critical Point, for All of the DHB Complexes Calculated

	CH_3OH			TFE			CF_3OH		
	BH_4^-	AlH_4^-	GaH_4^-	BH_4^-	AlH_4^-	GaH_4^-	BH_4^-	AlH_4^-	GaH_4^-
CT	0.030	0.037	0.036	0.052	0.066	0.064	0.120	0.152	0.152
MOP	0.174	0.174	0.195	0.242	0.242	0.273	0.321	0.475	0.448
WBI	0.024	0.047	0.044	0.039	0.076	0.071	0.100	0.191	0.181
ρ_c	0.025	0.026	0.026	0.032	0.035	0.034	0.053	0.063	0.062
$\nabla^2\rho_c$	−0.014	−0.013	−0.012	−0.016	−0.013	−0.013	−0.011	−0.004	−0.004

Table 3. Energy Values for the DHB Interactions (kcal/mol)

	CH_3OH			TFE			CF_3OH		
	BH_4^-	AlH_4^-	GaH_4^-	BH_4^-	AlH_4^-	GaH_4^-	BH_4^-	AlH_4^-	GaH_4^-
ΔE	−12.7	−10.7	−10.5	−19.3	−17.0	−17.0	−24.9	−21.8	−21.5
ΔE_{BSSE}	−12.5	−10.5	−10.3	−19.0	−16.9	−16.7	−24.6	−21.6	−21.2
ΔE + ZPVE	−12.0	−10.1	−10.1	−19.0	−16.0	−16.0	−24.7	−22.2	−22.0
ΔE(THF)[a]	−4.2	−4.0	−3.7	−5.3	−5.2	−5.0	−8.9	−8.5	−7.7
E_{HH}[b]	−4.4	−4.4	−4.3	−6.2	−6.6	−6.4	−12.8	−15.5	−14.8
$\Delta H(\Delta\nu)$[c]	−6.1	−6.3	−6.2	−7.2	−7.7	−7.6	−11.2	−11.8	−11.8
ΔH_{exp}[d]	−4.1		−4.3	−5.2		−5.4			

[a] ΔE(THF) calculated in THF as a solvent by CPCM. [b] E_{HH} is the energy of the hydrogen bond, calculated using the AIM method.[37] [c] ΔH calculated using the computed $\Delta\nu_{OH}$ using Iogansen's equation.[47] [d] From refs 13a,b and 17.

proton donor acidity, with the tendency being in line with the shortening of the H···H distance. Wiberg bond indexes (WBIs)[34] are in the range 0.024−0.191, indicating, as expected, the partial covalent character of the dihydrogen bond. For a given alcohol, they increase in the same order, $BH_4^- < GaH_4^- \leq AlH_4^-$, which is consistent with the decrease in the H···H bond lengths.

In recent years, numerous works have been published about Bader's AIM theory[43] application for studying hydrogen bonds, with the characteristics of the hydrogen-bond critical point being the most frequently used features to distinguish from other types of interactions.[44] In particular, it has been detected many times that the electron density at hydrogen-bond critical point ρ_c and its Laplacian $\nabla^2\rho_c$ correlate well with the hydrogen-bond energy.[45] The AIM methodology was also applied to the study of DHB systems.[46] In the present study, H···H bond critical points (3, −1) were found for all of the DHB complexes studied. The electron density at the critical point (ρ_c) varies from 0.025 to 0.063, with the values being comparable to those previously reported for DHB complexes.[46] The ρ_c values obtained are little sensitive to the nature of the central main-group atom, slightly increasing in the above-discussed order B < Ga ≤ Al. On the contrary, ρ_c increases significantly with the proton donor strength. Interestingly, in contrast to the previous findings for DHB systems,[46] in the present case of anionic group 13 hydrides, the values of the Laplacian of the electron density at the H···H bond critical point are negative, ranging from −0.014 to −0.004. The negative values of Laplacians indicate the presence of the electronic charge between the two interacting hydrogen atoms and a slight covalency along the H···H interaction in these negative charge-assisted hydrogen bonds.

DHB Energy. The energies for the DHB interaction gathered in Table 3 were calculated as the differences between the energy of the complex and the energies of isolated reactants. The experimentally determined values[17] are also given. MP2 calculations performed for the DHB complexes of BH_4^- with CH_3OH and CF_3OH and GaH_4^- with CH_3OH give slightly higher complexation energy

(44) Sobczyk, L.; Grabowski, S. J.; Krygowski, T. M. *Chem. Rev.* **2005**, *105*, 3513−3560.
(45) (a) Rozas, I.; Alkorta, I.; Elguero, J. *J. Am. Chem. Soc.* **2000**, *122*, 11154−11161. (b) Pacios, L. F. *J. Phys. Chem. A* **2004**, *108*, 1177−1188.
(46) (a) Alkorta, I.; Elguero, J.; Foces-Foces, C. *J. Chem. Soc., Chem. Commun.* **1996**, 1633−1634. (b) Grabowski, S. J. *J. Phys. Chem. A* **2000**, *104*, 5551−5557.

values, with ΔE(MP2) being −14.2, −25.0, and −11.3 kcal/mol, respectively. Inclusion of the zero point vibrational energies has very little influence on the interaction energies ($\Delta\Delta E \sim 0.6$ kcal/mol) or the basis-set superposition error (BSSE) correction (maximum BSSE value obtained is 0.3 kcal/mol). The ΔE values obtained for AlH_4^- and GaH_4^- are very similar, whereas those for BH_4^- are slightly higher for all of the alcohols considered. Such changes (B > Al ≈ Ga) do not correspond to the experimental trend (B < Ga).[17] Unfortunately, the experimental data for the enthalpy of DHB to AlH_4^- are not yet available. The energy values obtained in the gas-phase range between −10.5 and −12.7 kcal/mol for CH_3OH, between −17.0 and −19.3 kcal/mol for TFE, and between −21.4 and −24.9 kcal/mol for CF_3OH. The more acidic the alcohol, the larger is the interaction energy.

The inclusion of solvent effects (THF) by CPCM in the calculation has a dramatic effect on the computed DHB energies: taking into account the solvent polarity leads to a considerable (ca. 3 times) decrease of the interaction energies (Table 3), which become much closer to the experimental values. The difference between computed ΔE(THF) and experimental energy values is lower than 0.6 kcal/mol although the trend is the same as that in the gas phase (B > Al ≈ Ga). Note that solvent effects are more pronounced in the present case of anionic main-group hydrides than in the case of neutral transition-metal hydrides.[5c,d,6,8,9,41] Despite the above-mentioned change in the geometries after optimization in THF, the absolute energies in THF of the solvent- and gas-phase-optimized DHB adducts are similar, showing a difference of only 0.4 kcal/mol, whereas the complexation energies ΔE(THF) with and without optimization differ by only 0.2 kcal/mol. Thus, we are confident that single-point-energy-only calculations at the gas-phase-optimized geometries give a good estimation of the interaction energies in solution.

The energy of the H···H interactions was also estimated using the correlation between the energy of the contact (E_{HH}) with the value of the potential energy density function $V(r)$ in the corresponding bond critical point (3, −1): $E_{HH} = (1/2)V(r)$ proposed by Espinosa et al.[37] for A−H···O hydrogen bonds. Examples of the experimental validation of this approach for classical hydrogen bonds can be found in the literature.[48] The E_{HH} energies calculated are close to the experimental data (Table 3), and their dependence on the central element for stronger proton donors (TFE and CF_3OH) is in agreement with the experimental trend.[17]

The hydrogen-bond enthalpies $\Delta H(\Delta\nu)$ were also determined according to Iogansen's empirical correlation equation $-\Delta H^\circ = 18\Delta\nu/(720 + \Delta\nu)$,[47] introducing the computed $\Delta\nu_{OH}$ in the equation. These values reasonably compare with the experimental values, although calculated values are always slightly higher than experimental ones.

(47) Iogansen, A. V. *Theor. Exp. Chem.* **1971**, *7*, 312−317.
(48) (a) Lyssenko, K. A.; Korlyukov, A. A.; Antipin, M. Yu. *Mendeleev Commun.* **2005**, 90−93. (b) Kozlov, V. A.; Odinets, I. L.; Lyssenko, K. A.; Churusova, S. G.; Yarovenko, S. V.; Petrovskii, P. V.; Mastryukova, T. A. *Heteroatom Chem.* **2005**, *16*, 159−168. (c) Gatti, C.; May, E.; Cargnoni, F. *J. Phys. Chem. A* **2002**, *106*, 2707−2720.

Table 4. EDA for DHB Complexes (in kcal/mol)

EH_4/ROH	E_{ES}	E_{EX}	E_{PL}	E_{CT}	E_{MIX}	ΔE	PL/ES	CT/ES
BH_4/CH_3OH	−12.5	5.7	−3.5	−2.0	1.7	−10.7	0.28	0.16
AlH_4/CH_3OH	−11.3	5.8	−2.4	−2.0	1.2	−8.7	0.21	0.18
GaH_4/CH_3OH	−11.7	7.5	−3.9	−3.7	1.0	−10.9	0.34	0.32
BH_4/TFE	−23.0	9.2	−7.0	−3.4	4.3	−20.0	0.30	0.15
AlH_4/TFE	−19.7	9.4	−3.8	−3.7	2.0	−15.9	0.19	0.19
GaH_4/TFE	−20.6	10.5	−4.6	−5.2	1.3	−18.6	0.22	0.25

These results show that the interaction energies mainly depend on the nature of the alcohol, whereas the nature of the hydride has a smaller effect on the interaction energies.

EDA. A decomposition of the molecular interaction energy into components is very useful for an understanding of the fundamental nature of the interaction. An approach for doing this was introduced by Kitaura and Morokuma[39] in which the electrostatic component (E_{ES}) represents the classical Coulombic force between the undisturbed charge distributions of the two partner molecules. The exchange repulsion (E_{EX}) is the short-range repulsion that arises from the overlap of the monomer charge clouds. The remaining components arise when the two molecules are permitted to perturb the electron clouds of one another. The polarization (E_{PL}) and charge-transfer (E_{CT}) terms represent the energetic consequences of electronic redistributions that occur within the confines of a single molecule and of transfer of the electrons from one molecule to the other, respectively. The mixing (E_{MIX}) or coupling term arises from the fact that the above four interactions are not strictly independent of each other. Herein the Kitaura−Morokuma decomposition analysis of the DHB energy contributions was carried out for CH_3OH and TFE adducts of all three EH_4^- complexes. The total interaction energies (ΔE) collected in Table 4 show some differences with the values presented in the Table 3 because of the need for using a different basis set [6-31++G(d,p) instead of 6-311++G(d,p); see the Computational Details section). However, despite these small differences in ΔE, the relative contributions of all of the energy components are the same in both basis sets, as was verified for DHB complexes of the boron hydride.

Among the different terms, the electrostatic contribution (E_{ES}) is the largest one. The exchange repulsion (E_{EX}) is twice as small in magnitude; thus, the sum of the ES and EX terms is considerably attractive. The contributions of polarization (E_{PL}) and charge-transfer (E_{CT}) terms depend on the central element of the hydride (see Table 4). The contribution of the PL term in the case of BH_4^- is significantly larger than that of the CT term. Substitution of boron by aluminum and gallium leads to the leveling of these components. Thus, the comparison of the relative PL/ES and CT/ES quotients indicates that the first term for BH_4^- is about twice as large as the second, whereas for AlH_4^- and GaH_4^-, the values of PL/ES and CT/ES are similar. It is noteworthy that the CT/ES values increase down the group: B < Al < Ga. The polarization energy term, PL, does not show such a clear trend; in fact, its relative contribution depends on the alcohol.

The greatest role of the electrostatic term in the energy of the DHB complexes of group 13 tetrahydrides is similar to that of the DHB complexes of transition-metal hydrides as

Table 5. Calculated ν(EH) Band Positions (in cm^{-1}) and Frequency Shifts for DHB Complexes (in Parentheses) with Respect to Free EH_4^-

	BH_4^-		AlH_4^-		GaH_4^-	
	ν(E−H)	$\Delta\nu$(E−H)[c]	ν(E−H)	$\Delta\nu$(E−H)[c]	ν(E−H)	$\Delta\nu$(E−H)[c]
	2263[a]		1732[a]		1762[a]	
	2230[b]		1644[b]		1685[b]	
CH_3OH	2300	(53.5)	1761	(73)	1784	(60.5)
	2286	(39.5)	1689	(1)	1725	(1.5)
	2279	(32.5)	1683	(−5)	1717	(−6.5)
	2216	(−30.5)	1651	(−37)	1660	(−63.5)
TFE	2334	(87.5)	1774	(86)	1807	(83.5)
	2300	(53.5)	1717	(29)	1762	(38.5)
	2289	(42.5)	1692	(4)	1728	(4.5)
	2198	(−48.5)	1636	(−52)	1634	(−89.5)

[a] A_1 mode. [b] T_2 mode. [c] With respect to the mean of A_1 and T_2 modes, ν'(E−H): $\Delta\nu(E-H) = \nu(E-H)^{complex} - \nu'(E-H)$.

well as of classical hydrogen bonds of organic bases.[5c] The increase of the polarization energy component for the DHB adduct of the main-group hydrides is similar to that of the transition-metal hydrides.[42a] The classical hydrogen bond is largely electrostatic in origin, with much smaller attractive contributions from polarization and charge transfer: ES ≫ CT > PL (recent examples of the EDA for the model systems HNO···HX and NH_3···NH_3 can be found in ref 42). For the model H···H complexes of LiH with HF or H_2O, the classification is somewhat different, ES > CT ≥ PL, because the PL contribution increases significantly.[42a] A very high contribution from the polarization energy (∼75% of the ES) has been found[42b] for the B−H···H−N dihydrogen bonds in the H_3BNH_3 dimer with a CT contribution of about 35% of ES. Here we found that for the boron hydride the energy components of the DHB complex can be termed in a similar manner, ES > PL > CT, whereas for the heavier aluminum and gallium analogues, this sequence is ES > PL ≥ CT. The high contribution from the polarization energy is connected with significant geometric distortion and considerable shift in the electron density within the interacting molecules.

Vibrational Analysis. The results of the frequency calculations for group 13 tetrahydrides with CH_3OH and TFE (stretching vibrations of E−H bonds) are presented in Table 5. The frequencies of both A_1 and T_2 modes depend on the central element, with the values changing within the group according to the following sequence: B > Ga > Al. The degeneracy of the second band of ν(E−H) stretching vibrations (T_2 mode) is naturally absent in the MH···HOR complexes. Therefore, four frequencies describe these stretches in DHB complexes. Three of these frequencies are shifted to higher values: these are assigned to the nonbonded ν(E−H) modes. The band shifted to the low-frequency range is assigned as $\nu(E-H)_{bonded}$.

The directions of bonded and nonbonded E−H frequency shifts upon the DHB complex formation are in agreement with the experimental IR spectral changes observed for DHB complexes for the gallium and boron hydrides.[17] They also match with the previously computed shifts for BH_4^- and GaH_4^- [17] and transition-metal hydrides.[5c] The IR spectra in solution demonstrate the overlap of free E−H vibrational bands due to the small frequency difference. So, the initial

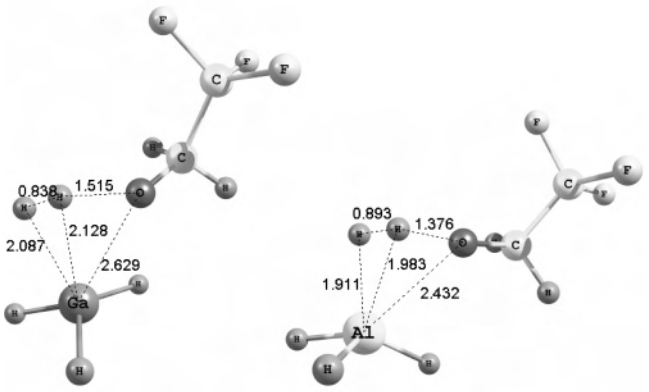

Figure 3. TSs for the alcoholysis reaction of GaH_4 and AlH_4 with TFE.

bands of ν(BH) for BH_4^- and ν(GaH) for GaH_4^- studied in solution (CH_2Cl_2 and THF) at 180−290 K have complex shapes and are observed at 2200 and 1700 cm^{-1}, respectively.[13a,b,17] In the presence of weak proton donors, the decrease in the intensity and some broadening of the ν(EH) bands, as well as the appearance of the low- and high-frequency shoulders (assigned to the one bonded and three nonbonded E−H stretching vibrations of DHB), were observed. The $\Delta\nu$(GaH) values for DHB complexes of GaH_4^- with weak proton donors[17] are larger than the $\Delta\nu$(BH) value for the boron analogue[13a,b] by about 10−30 cm^{-1}. The computed band shift values are in agreement with the experimental data. As expected, the calculated frequency shifts increase with the proton donor strength (Table 5).

II. Proton-Transfer Reaction. The mechanism for the reaction between group 13 hydrides and several alcohols (as proton donors) is discussed here. With one exception (the $BH_4^- + CF_3OH$ reaction), the proton transfer, H_2 elimination, and alkoxo derivative formation take place in a single step. IRC calculations were carried out in both directions starting from the located TSs. No intermediates other than the DHB complexes were found for any of the systems except in the case of the $BH_4^- + CF_3OH$ reaction. The structures of the TSs and products are qualitatively similar for all of the systems (see, for instance, Figure 3).

The geometrical parameters of the TSs found are collected in Table 6. The TSs can be described as dihydrogen complexes, as proven by the H···H distances spanning a range between 0.769 and 0.981 Å. The O···H(H) and O···E distances are significantly shorter than the sum of the vdW radii, therefore indicating the strong interaction between the OR^- anion and the partly positive hydrogen atom of the side-on η^2-H_2 ligand and additional interaction between the E and oxygen atoms. Thus, for instance, the O···E distance for the TS of GaH_4^- with the weakest alcohol (CH_3OH) is 2.444 Å, whereas the sum of the vdW radii is 3.4 Å. The increase of the proton donor strength (TFE instead CH_3OH) leads to the contraction of the H···H bond; for example, in the GaH_4^- TS, the H···H distance shortens from 0.921 to 0.838 Å. Opposite trends are observed for the O···H distances in the TS; for instance, in the case of the GaH_4^- TS, the O···E distance lengthens from 2.444 to 2.629 Å upon substitution of CH_3OH by TFE.

Table 6. Geometric Parameters (in Angstroms) of the TSs for the Reaction of EH_4^- with the Proton Donors ROH

	CH_3OH			TFE			CF_3OH		
hydride	H···H	H···E	H···O/E···O	H···H	H···E	H···O/E···O	H···H	H···E	H···O/E···O
BH_4^-	0.838	2.227, 2.178	1.535/2.681	0.793	2.287, 2.249	1.721/2.832	0.891 (TS1) 0.755 (TS2)	1.310, 1.626 2.584, 2.583	1.467/3.010 2.132/3.284
AlH_4^-	0.981	1.962, 1.989	1.244/2.232	0.893	1.911, 1.983	1.376/2.432	0.780	2.080, 1.990	1.802/2.877
GaH_4^-	0.921	2.131, 2.130	1.325/2.444	0.838	2.087, 2.128	1.515/2.629	0.769	2.188, 2.299	1.857/3.028

Table 7. Relative Energies (in kcal/mol) for DHB Complexes, TSs, and Products of the Reaction of EH_4^- Hydrides with Alcohols[a]

	BH_4^-			AlH_4^-			GaH_4^-		
ROH	DHB	TS	product	DHB	TS	product	DHB	TS	product
CH_3OH	−12.7 (−4.2)	42.5 (53.2)	−11.6 (−1.7)	−10.7 (−4.0)	16.6 (20.4)	−24.0 (−17.4)	−10.5 (−3.7)	23.6 (29.3)	−11.7 (−4.0)
TFE	−19.3 (−5.3)	26.4 (41.7)	−21.6 (−5.8)	−17.0 (−5.2)	5.5 (16.1)	−33.8 (−21.2)	−17.0 (−5.0)	10.1 (21.6)	−22.5 (−8.8)
CF_3OH	−24.9 (−8.9)	−20.7/−6.6[b] (−6.3/8.0)[b]	−34.5 (−17.2)	−21.8 (−8.5)	−16.5 (−7.6)	−48.1 (−34.8)	−21.5 (−7.7)	−13.9 (−4.7)	−39.1 (−25.6)

[a] In parentheses are relative energies in THF. The energy of the separated EH_4^- + ROH is taken as a zero of energies. [b] Relative energies of TS1 and TS2, respectively.

The H−H bond distances for the TS lengthen in the order B < Ga < Al. The strength of the H···O hydrogen bonds and of the forming E···O coordination bonds mainly affects these variations; the decrease of the H···O and E···O distances in the sequence B > Ga > Al leads to the lengthening of the H−H bond.

Transition-metal dihydrogen complexes have H−H distances ranging from 0.8 to 1.0 Å.[3,27] Hundreds of these complexes have been reported as isolable species because of the existence of combined forward- and back-donation, which is not possible in the main-group hydrides. Contrarily to what happens with transition-metal hydrides, in main-group hydrides the dihydrogen complexes are not stable. For this reason, they are found as TSs in the protonation reaction instead of intermediates. The existence of weakly bound $MH_3(\eta^2\text{-}H_2)$ complexes for group 13 elements has been postulated.[10] $AlH_3(\eta^2\text{-}H_2)$ has been theoretically characterized as a minimum by CCSD calculations.[29] In this species, the H−H distance of the H_2 ligand is significantly shorter (0.750 Å) than those found for the TSs of AlH_4^- protonation (0.780−0.981 Å; Table 6). In our calculation, the isolated $GaH_3(\eta^2\text{-}H_2)$ species (without a counteranion) with the side-on (η^2-H_2) ligand, is also found as a minimum, showing the H−H distance of 0.750 Å, which is only a little longer than that in the H_2 molecule (0.742 Å) and appreciably shorter than those found in the TSs (0.769−0.921 Å). For the boron analogue, such a dihydrogen complex was predicted theoretically and observed experimentally by IR matrix isolation.[28] The possibility of this dihydrogen complex existence at low temperature is probable due to the tighter coordination of the H−H ligand with boron: the distances of (H)H···B (1.422 and 1.433 Å) in $BH_3(\eta^2\text{-}H_2)$[26] are about twice shorter than those in $GaH_3(\eta^2\text{-}H_2)$ (Ga···H = 2.471 and 2.454 Å) and $AlH_3(\eta^2\text{-}H_2)$ (Al···H = 2.295 and 2.331 Å).[27] It is noteworthy that the H−H (0.799 Å) distance in $BH_3(\eta^2\text{-}H_2)$ is also significantly shorter than that in the corresponding TS (Table 6).

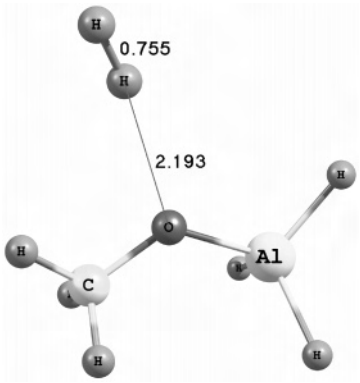

Figure 4. Structure of the reaction product H_3AlOCH_3.

The reaction products can be described as vdW complexes $[H_3EOR^-]\cdot H_2$ with a very weak interaction between the dihydrogen and oxygen (see, for example, Figure 4) and have many common features. The E−H distances decrease in comparison to those in the corresponding initial hydrides. The M−O bond lengths increase down the group: B < Al < Ga. Their values range from 1.511 to 1.930 Å, from 1.529 to 1.953 Å, and from 1.598 to 2.031 Å for CH_3OH, TFE, and CF_3OH, respectively. The O···H_2 distances range between 2.145 and 2.843 Å, being very close to the sum of the vdW radii (2.6−2.8 Å).

Thus, comparative analysis shows that proton transfer, H_2 elimination, and alkoxo derivative formation occur after DHB formation in a concerted way. The single exception is for the reaction between CF_3OH and BH_4^-, which is found to be stepwise with the formation of a $BH_3(\eta^2\text{-}H_2)\cdots OR^-$ intermediate (see below).

The relative energies of all of the species associated with the reaction profile are presented in Table 7, with the energy of the separated MH_4^- + ROH being taken as a zero of energies. The reaction is strongly exothermic for all systems. Starting from the DHB complexes, the energy barriers for the process are quite different depending on the nature of the hydride and alcohol (Table 8). Negative relative energy values found for the TSs in the reaction with CF_3OH are due to their great stability compared to separated reactants; in any case, activation barriers are positive because the initial DHB complexes are even more stable. The barrier heights are lower when the alcohol is a better proton donor. The high barriers obtained for the interaction of BH_4^- with CH_3OH and TFE agree with the experimentally observed

Table 8. Energy Barriers (in kcal/mol) for the Alcoholysis Reaction[a]

	BH_4^-		AlH_4^-		GaH_4^-	
ROH	forward	backward	forward	backward	forward	backward
CH_3OH	55.2 (57.4)	54.1 (54.9)	27.3 (24.4)	40.6 (37.8)	34.1 (33.0)	35.3 (33.3)
TFE	45.7 (47.0)	48.0 (47.5)	22.5 (21.3)	39.3 (37.3)	27.1 (26.6)	32.6 (30.4)
CF_3OH	18.3[b] (16.9)[b]	27.9[b] (25.2)[b]	5.3 (0.9)	31.6 (27.6)	7.6 (3.0)	25.2 (20.9)

[a] In parentheses are relative energies in THF. [b] Energy barriers from DHB and product to TS2.

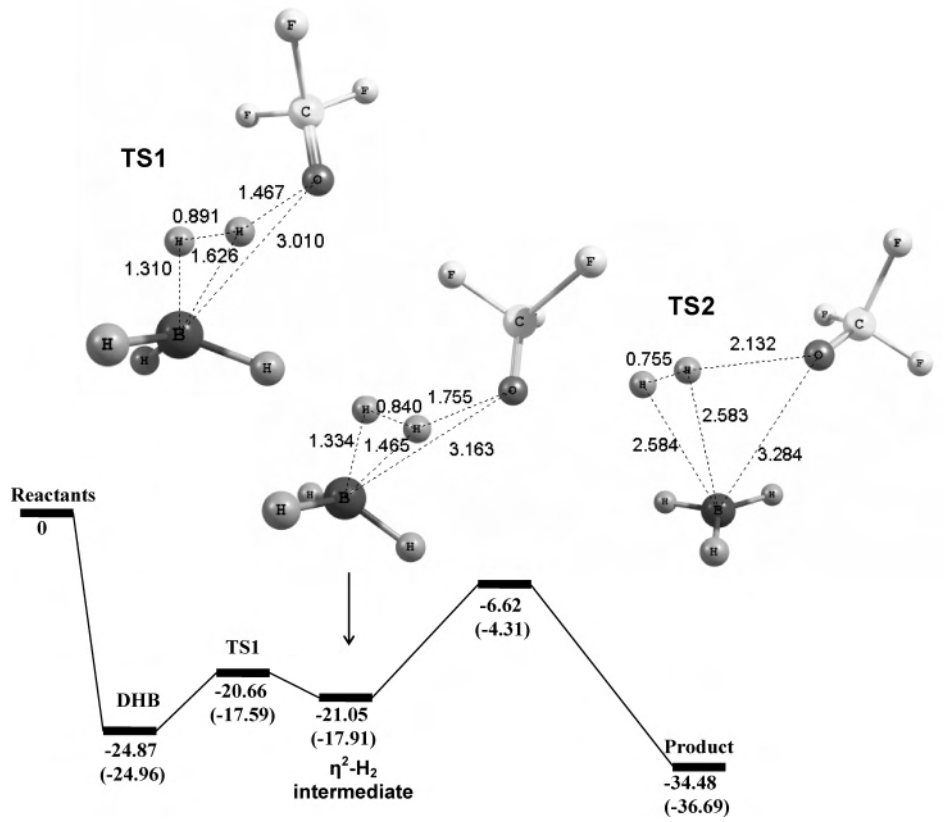

Figure 5. B3LYP energy profile for the reaction of BH_4 with CF_3OH. In parentheses are the MP2 relative energies.

DHB formation and the absence of proton transfer in the case of methanol and slow reaction with TFE at room temperature.[13] The considerable decrease of the proton-transfer barrier on going from TFE to CF_3OH is not surprising because the latter is a significantly stronger acid.[6,49] For a given alcohol, the activation barriers decrease in the order B > Ga > Al and are always remarkably higher for the boron than for the gallium or aluminum hydrides. This is in line with the higher reactivity of gallium than boron hydride; the proton transfer and H_2 elimination have been observed for GaH_4^- with FCH_2CH_2OH or indole even at low temperatures (>230 K).[17]

The energy profile calculated for the reaction between BH_4^- and CF_3OH is presented in Figure 5. The structures of the two TSs and the intermediates are also depicted. The first reaction step consists of the formation of the DHB complex described in the previous section. The next step accounts for the hydride protonation with the formation of the postulated $BH_3(\eta^2\text{-}H_2)$ intermediate. The energy barrier for this step is only 4.2 kcal/mol. The second step can be assimilated to a "ligand substitution" using transition-metal chemistry words, where the H_2 is substituted by the alkoxo group, releasing H_2 and forming the alkoxoboron final product. The energy barrier for this step is 14.4 kcal/mol.

The MP2/6-311++G(d,p) study of the reaction between BH_4^- and CF_3OH reveals the same energy profile as that presented in Figure 5, with only a slight difference in the energies and geometries of the intermediates (see the Supporting Information for details). Furthermore, calculation of the proton transfer for the BH_4^-/CH_3OH system at the MP2 level shows the same profile as that at the B3LYP level with only one TS and no intermediate other than the DHB complex.

The last point we address is how the solvent affects the relative energies of all of the species on the reaction pathway. To provide a comprehensive comparison, a single-point calculation of the energies of the separated reactants, DHB adducts, TSs, and products has been performed in THF by the CPCM method, at the gas-phase-optimized geometries. The solvent destabilizes all of the species (DHB, TS, and products) with respect to the separated reactants (EH_4^- + ROH). This behavior can be clearly appreciated from the

(49) Huey, L. G.; Dunlea, E. J.; Howard, C J. *J. Phys. Chem.* **1996**, *100*, 6504−6508.

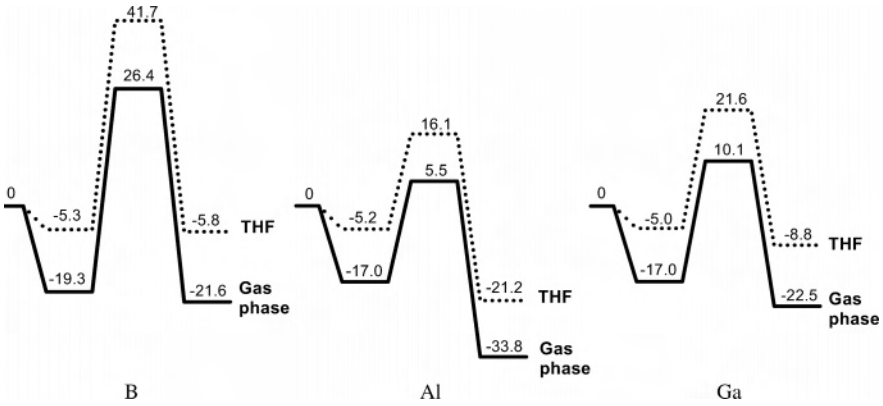

Figure 6. Energy profiles for the reaction of EH_4 hydrides with TFE in the gas phase and in THF.

gas-phase and THF energy profiles for the reactions with TFE depicted in Figure 6. The effect of the central atom is also apparent from Figure 6.

Notably, the sequence of the activation barriers in THF (B > Ga > Al, CH_3OH > TFE > TFE) is the same as that in the gas phase (Table 8). Activation barriers ($\Delta E^{\ddagger}$) for BH_4^- in the gas phase and in THF are very high, but the solvent effect is rather small, increasing the barrier only by 1.6 kcal/mol. This is due to very similar destabilization of the DHB intermediate and the TS. The activation barriers are about twice as low for the aluminum and gallium analogues ($\Delta E^{\ddagger}$ = 22.5 and 21.2 kcal/mol for Al and 27.1 and 26.6 kcal/mol for Ga in the gas phase and in THF, respectively). Thus, the solvent effect of THF diminishes $\Delta E^{\ddagger}$ in the cases of GaH_4^- and AlH_4^- reactions, but these changes are also very small (between −0.4 and −1.3 kcal/mol). Again THF destabilizes the DHB adducts and TSs by approximately the same extent. Previously, a decrease of the activation barrier of the proton transfer to the transition-metal hydride due to the solvent effect was obtained. The barrier decreases with an increase of the media polarity [$\Delta E^{\ddagger}$(gas phase) > $\Delta E^{\ddagger}$(heptane) > $\Delta E^{\ddagger}$(CH_2Cl_2)].[6] The main difference between the previously studied transition-metal hydrides and the present main-group hydrides is in the charge of the system. In the neutral transition-metal systems, the proton-transfer reaction entails the creation of charge, giving an ion pair, which is stabilized in polar media. In the anionic main-group hydrides, there is only a charge migration, and thus the media effects are smaller. The activation barriers of the reverse processes (Table 8) are considerably higher than those of the direct processes, making the protonation reactions irreversible. The influence of THF on the activation barriers of the reverse process is also small.

Conclusions

The theoretical study of the interaction of the group 13 hydrides EH_4^- with proton donors of different strength by means of DFT/B3LYP and MP2 methods yields similar results, independent of the computational methodology used, which are in agreement with the experimental data available. A comparison with the studies of proton-transfer reactions of transition-metal hydrides having more precedents shows that DHB intermediate formation preceding the proton transfer is a common feature for both types of hydrides. The structural characteristics of DHB complexes show many similar features: a short H···H distance, linearity of the H···HO moieties, elongation of the interacting M−H/E−H and O−H bonds, medium-strength energies, and a major contribution of the electrostatic energy term to the total interaction energy. However, the dependence of the structural and energetic characteristics of DHB complexes on the central element obtained here is weaker than that in the case of the group VIII transition-metal hydrides previously studied by some of us. The mechanistic aspects of the proton-transfer reaction present many important differences. Proton transfer to hydride hydrogen of transition-metal complexes results in the DHB complex formation as a product or intermediate; the reversibility of the reaction was shown. For the unstable dihydrogen complexes, the next step of the reaction is either isomerization into a classical transition-metal hydride or H_2 evolution leading to the alkoxo derivative formation. The very low stability of the main-group (η^2-H_2) complexes (due to their incapability to back-donate) changes their role in proton-transfer reactions from intermediates to TSs. The (η^2-H_2) species, though stabilized by a hydrogen bond with the OR− anion (similar to cationic nonclassical transition-metal hydrides), were found only as the TSs for the reactions of boron, aluminum, and gallium tetrahydrides with alcohols. The reaction has concerted character, with the proton transfer, H_2 release, and alkoxo derivative formation occurring in a single step. Only the BH_4^-/CF_3OH system presents a different mechanism, with a shallow minimum for the DHB complex. The activation barriers [both in the gas phase and in the solvent (THF)] are very high for boron tetrahydride, preventing its alcoholysis by TFE and weaker proton donors. The barriers decrease dramatically for aluminum and gallium species, with the $\Delta E^{\ddagger}$ of AlH_4^- alcoholysis being the lowest in the group. Moreover, the reactions of AlH_4^- with alcohols (in the gas phase and in THF) are much more favorable than those of the boron and gallium analogues, explaining the high reactivity of alumohydride in protic media. In all cases, the activation barriers of the reverse processes are considerably higher, making H_2 loss and alkoxo derivative formation irreversible. Thus, our results show the resemblance of DHB complexes of main-group and transition-metal hydrides and differences in the mechanistic aspects of the proton transfer

in these systems, providing a better understanding of the trends in main-group hydride reactivity.

Acknowledgment. We thank EC for promoting this scientific activity with financial support through the Marie Curie Research Training Network Program "Hydrochem" (Contract HPRN-CT-2002-00176). This work was also supported by the Russian Foundation for Basic Research (Grant 04-03-32456), the Fundamental Research Program of Presidium of RAS, Russian Federation President Grant MK-3886.2005.3, and Spanish MEC (Project CTQ2005-09000-CO2-01). The use of the computational facilities of the Centre de Supercomputació de Catalunya is greatly appreciated.

Supporting Information Available: Tables of optimized geometries (Cartesian coordinates) for the calculated species. This material is available free of charge via the Internet at http://pubs.acs.org.

IC052028N